JOURNAL OF MATERIALS SCIENCE 23 (1988) 2712–2722

An investigation of grain boundary sliding in superplasticity at high elongations

ZHAO-RONG LIN*, ATUL H. CHOKSHI‡, TERENCE G. LANGDON
Departments of Materials Science and Mechanical Engineering, University of Southern California, Los Angeles, California 90089-1453, USA

Experiments were performed on the superplastic Zn–22% Al eutectoid alloy to determine the contribution of grain boundary sliding at both low (35%) and high (~235%) elongations. The tests were conducted at two different strain rates in the superplastic Region II, and the results show that, within the accuracy of the measurements, there is a large sliding contribution at both elongations. By taking detailed measurements of both the magnitude of the sliding offset and the type of interface, it is shown that the average offsets are generally a maximum at the Zn–Zn boundaries, there is less sliding at the Zn–Al interfaces, and the offsets are a minimum at the Al–Al boundaries. In addition, the distributions of the magnitudes of the sliding offsets are similar at both the low and high elongations. It is concluded that grain boundary sliding is an important deformation process in the superplastic Region II and that it remains important even when the elongation is very high. The nature of the results indicates also that experimental observations of the deformation behaviour in superplastic materials at low elongations (up to 50%) provide meaningful information on the behaviour at much higher (superplastic) elongations.

1. Introduction

When a superplastic material is tested in tension, the steady-state flow stress, σ, is related to the imposed strain rate, $\dot{\varepsilon}$, through an expression of the form

$$\sigma = B\dot{\varepsilon}^m \quad (1)$$

where m is termed the strain rate sensitivity and B is a constant which depends on temperature and grain size.

Superplastic materials generally exhibit a sigmoidal relationship in a logarithmic plot of σ against $\dot{\varepsilon}$, such that the values of m are low (~0.2) at low strain rates, high (~0.5) at intermediate strain rates and low (~0.2) at high strain rates. Since the total elongation to failure increases with increasing strain rate sensitivity, both experimentally [1] and theoretically [2], the elongations are high at intermediate strain rates (typically over about two orders of magnitude of strain rate) and the elongations drop to much lower values when the strain rate is either decreased or increased outside this optimum range. The range of strain rates where m is high and there is optimum superplasticity is termed Region II, and the regions where m decreases at the lower and higher strain rates are termed Regions I and III, respectively.

Superplasticity requires a very small grain size, typically less than ~10 μm, and it is generally considered that the grain boundaries play an important role in superplastic deformation [3]. To date, many experiments have been conducted to determine the significance of grain boundary sliding in the three regions of flow using several different superplastic alloys. These experiments have been conducted by taking measurements of the offsets in marker lines at grain boundaries and then calculating the sliding contribution ξ as a percentage, where ξ is equal to the ratio $\varepsilon_{gbs}/\varepsilon_t$ where ε_{gbs} is the strain due to grain boundary sliding and ε_t is the total strain.

Table I summarizes the values of ξ published to date in the three regions of flow associated with superplasticity, together with the mean linear intercept grain size of each material, $\bar{L}$, the testing temperature, and the elongation at which the sliding measurements were taken, $\Delta L/L_0$, where ΔL is the increase in length and L_0 is the initial gauge length.†

Inspection of Table I shows that, with the exception only of the experiments on Zn–22% Al by Shariat *et al.* [20], the values reported for ξ are in remarkable agreement. First, the values of ξ in the superplastic Region II are consistently high, ranging from a minimum of 44% [9, 10] to a maximum of ~80% [7, 21], thereby indicating that the sliding process makes a major contribution (of the order of ~50 to 70%) in the region of maximum superplasticity. Second, the

*On leave from Mechanical Engineering Department, Nanjing Aeronautical Institute, Nanjing, Jiang-su 210002, People's Republic of China.
‡ *Present address*: Division of Materials Science and Engineering, Department of Mechanical Engineering, University of California, Davis, CA 95616, USA.
† Table I includes all published data for values of ξ in superplastic materials having very small grain sizes. It excludes measurement of ξ in the Al–4% Ge alloy [23] because, although this material was claimed to exhibit superplasticity, the elongations to failure were low (< 300%) and the grain size of the material was 80 μm.

0022–2461/88 $03.00 + .12

TABLE I Measurements of grain boundary sliding in Regions I, II and III of superplasticity

Material	Grain size, $\bar{L}$ (μm)	Testing temperature (K)	Elongation, $\Delta L/L_0$ (%)	ξ (%)			Reference
				I	II	III	
Al–33% Cu	~10.0	793	40	–	~70	–	Hori *et al.* [4]
Al–6.3% Mg–0.5% Mn	4.7	693	30	48 ± 5	65 ± 7	35 ± 4	Valiev *et al.* [5]
Al–9% Zn–1% Mg	9.3	793	60	42	63	26	Matsuki *et al.* [6]
Al–11% Zn–0.9% Mg–0.3% Zr	7.6	823	30	~60	~80	~50	Matsuki *et al.* [7]
Al–11% Zn–0.9% Mg–0.3% Zr	8.3	733 to 793	25	–	65 ± 7	~30	Matsuki *et al.* [8]
Cu–2.8% Al–1.8% Si–0.4% Co	4.5	823	10	28 ± 12	44 ± 10	20 ± 5	Shei and Langdon [9]
Cu–21% Zn–4% Al	7	873	25	38	44	36	Portnoy and Kozhanov [10]
Mg–4.3% Al–1.0% Zn–0.4% Mn	13.4	648	20	35	58	19	Puquan and Min [11]
Mg–33% Al	10.6	673	17	12	64	29	Lee [12]
Mg–1.5% Mn–0.3% Ce	9.6	673	30	33 ± 4	49 ± 6	30 ± 4	Valiev and Kaibyshev [13]
Pb–62% Sn	–	293	–	–	~70	–	Dingley [14]
Pb–62% Sn	9.7	423	22	21 ± 5	56 ± 12	20 ± 4	Vastava and Langdon [15]
Pb–62% Sn	6.0	293	15 to 25	–	~50	–	Furushiro and Hori [16]
Zn–0.4% Al	1.0	293	20	~40	~50	~30	Kaibyshev *et al.* [17]
Zn–22% Al	1.8	523	20	~30	~60	~30	Holt [18]
Zn–22% Al	1.6	523	20	<30	~60	<20	Novikov *et al.* [19]
Zn–22% Al	3.8	473	100	10 ± 5	11 ± 5	6 ± 3	Shariat *et al.* [20]
Zn–22% Al	0.9 to 3.9	473	20	–	~80	–	Motohashi and Shibata [21]
Zn–0.9% Cu–0.6% Mn	4.8	523 to 583	~25	–	67 ± 6	–	Matsuki *et al.* [22]

values of ξ in Regions I and III are consistently lower than in Region II, showing that sliding decreases in importance at the strain rates where the overall elongations are reduced.

A close examination in Table I shows, however, that all of these values of ξ were obtained at low specimen elongations, typically of the order of 20 to 30%. To overcome this limitation, Shariat *et al.* [20] took measurements of the sliding offsets in specimens of the Zn–22% Al eutectoid alloy deformed to an elongation of 100%. The results are shown in Table I, and it is instructive to note that the value of ξ is reduced to $11 \pm 5\%$ in Region II at $\Delta L/L_0 = 100\%$. This value contrasts with two earlier reports of $\xi \simeq 60\%$ in the same alloy in Region II at an elongation of only 20% [18, 19].

Shariat *et al.* [20] suggested that the very low values obtained for ξ were not a true representation of the specimen behaviour. Instead, it was noted that there are two limitations associated with measurements of ξ at high specimen elongations due to (i) the increase in the surface area as the specimen deforms and (ii) a limit imposed on the maximum values of the measured sliding offsets before the grains become separated and sliding becomes indeterminate. Thus, Shariat *et al.* [20] concluded that, despite the low value of ξ determined experimentally in Region II at an elongation of 100%, there was no true diminution in the contribution from sliding at high specimen elongations.

An opposing view was presented contemporaneously by Motohashi and Shibata [21]. In their experiments, conducted also on the Zn–22% Al eutectoid alloy, they obtained $\xi \simeq 80\%$ at a specimen elongation of 20% and, although they reported no direct measurements of ξ at high specimen elongations, they noted an apparent decrease in the evidence for grain boundary sliding at elongations above $\sim 100\%$. They concluded that grain boundary sliding is the predominant deformation mode in superplasticity at elongations up to $\sim 50\%$, but thereafter they suggested that sliding decreases in importance and the major deformation mode in Zn–22% Al changes to elongation of the zinc-rich phase controlled by zinc diffusion.

Although the experimental results of Shariat *et al.* [20] and Motohashi and Shibata [21] are qualitatively similar, because of the apparent decrease in sliding at elongations of $\sim 100\%$, there is a sharp dichotomy in the interpretation. The present research was therefore motivated by the realization that it is not possible at the present time to distinguish directly between these two opposing viewpoints, and the primary objective of this work was to carefully determine ξ both at low specimen elongations and at elongations of $> 200\%$.

A second objective was to investigate the variation of sliding with the type of interface. In the earlier study by Shariat *et al.* [20], it was reported that maximum sliding occurs on the Zn–Zn intercrystalline boundaries at 100% elongation, there is slightly less sliding on the Zn–Al interphase boundaries, and sliding is a minimum on the Al–Al intercrystalline boundaries. Thus, the present experiments were designed to check whether this behaviour occurs also at elongations in excess of 200%.

2. Experimental materials and procedure

Following Shariat *et al.* [20] and Motohashi and Shibata [21], the experiments were conducted on a two-phase eutectoid alloy containing a 22 wt % aluminium-rich α-phase and a 78 wt % zinc-rich β-phase. Sheets of the alloy, 2.54 mm in thickness and in a superplastic condition, were obtained from the New Jersey Zinc Co. The as-received grain size was about 1 μm, and a semi-quantitative spectrographic analysis revealed the following impurities in p.p.m.: Cr < 10, Cu 20, Fe 70, Mg < 10, Mn < 10 and Si 70.

Two tensile specimens were machined parallel to the rolling direction with gauge lengths of 6.4 mm. Each specimen was annealed in argon for 28 days at 523 K, and then furnace-cooled to produce a mean linear intercept grain size, measured along the tensile axis, of $\bar{L} \simeq 3.0 \pm 0.5\,\mu$m (equivalent to an initial spatial grain size, d ($= 1.74\bar{L}$), of $5.2 \pm 0.9\,\mu$m).* Prior to testing, each specimen was polished on emery paper, diamond paste and Al_2O_3 and MgO polishing compounds (to 0.05 μm), and then a series of marker lines, parallel to the tensile axis, was placed on the polished surfaces using 3 μm diamond paste on a lens tissue wetted with acetone.

Each specimen was pulled in tension using an Instron testing machine operating at a constant rate of crosshead displacement. The tests were performed at a temperature of 473 ± 1 K by immersing the specimens in an electrically heated bath of silicone oil stirred with bubbling argon. A period of one hour was allowed for temperature stabilization before tensile testing.

The two specimens were tested at initial strain rates of 1.33×10^{-2} and $1.33 \times 10^{-3}\,\text{sec}^{-1}$, respectively. Based on an earlier detailed study of the mechanical properties of Zn–22% Al [24], these rates lie within the superplastic Region II.

Each specimen was pulled to an elongation of 35%, and then it was removed from the oil bath, washed in acetone and placed in a scanning electron microscope. A series of photomicrographs was taken at different points along selected marker lines on the specimen surface, and these photomicrographs were used subsequently for the measurements of grain boundary sliding. The magnitudes of the offsets perpendicular to the stress axis, w, and the types of interface (whether Zn–Zn, Zn–Al or Al–Al) were recorded at every boundary intersected by a series of selected longitudinal marker lines. The average offset, $\bar{w}$, was estimated from measurements taken at 200 to 350 individual boundaries. As in the work of Shariat *et al.* [20], if the boundary appeared thickened because of the exposure of a boundary facet, the total offset was recorded by projecting the marker line across the interface. Finally, the value of ξ was calculated by putting $\varepsilon_t = \Delta L/L_0$

*This grain size is slightly smaller than in the experiments of Shariat *et al.* [20] where $\bar{L} \simeq 3.8 \pm 0.7\,\mu$m but the difference is not significant.

and estimating ε_{gbs} from the relationship [25]

$$\varepsilon_{gbs} = \phi \left(\frac{\bar{w}}{\bar{L}} \right)_l \quad (2)$$

where ϕ is a geometric factor and the subscript l refers to the procedure of taking measurements along the longitudinal tensile axis. Based on earlier experimental measurements in creep, and also the functional dependence of w on the angle between the grain boundary and the stress axis, the value of ϕ was taken as 1.5 [26].

Following these measurements, the specimen tested at the faster strain rate was returned to the testing machine and pulled to a total elongation of 196%. It was then removed from the machine and very carefully polished and scribed with a new set of longitudinal marker lines. Due to the fragile nature of the specimen at this stage of the experiment, it was decided to forgo the additional polishing and etching necessary for a determination of the grain size, and instead the testing was continued to a total elongation of 234%. A similar procedure was adopted for the second specimen except that the test was initially terminated at 200% and ultimately, after repolishing and scribing with a new set of marker lines, at a total elongation of 237%. Thus, these specimens were used to provide a direct measure of the sliding occurring in the increment of elongation from $\sim 200\%$ to $\sim 235\%$.

As at 35% elongation, measurements were taken on both specimens to determine the average sliding offset, $\bar{w}$, and again the magnitude of each offset was recorded as a function of the type of interface. Measurements were also taken along the longitudinal marker lines to determine the final mean linear intercept grain size, $\bar{L}_f$. The values of ε_{gbs} were then estimated from the relationship

$$\varepsilon_{gbs} = \phi (1 + \varepsilon_t) \left(\frac{\bar{w}}{\bar{L}_f} \right)_l \quad (3)^*$$

where ϕ was taken as 1.5 and ε_t was equal to the relative increment of strain after the repolish. Finally, these values were used to estimate ξ for the strain increment from $\sim 200\%$ to $\sim 235\%$.

3. Experimental results

3.1. Variation of ξ with elongation

Fig. 1 shows the surface features on the specimen tested at $1.33 \times 10^{-2}\,sec^{-1}$ to an elongation of 35%: the zinc-rich phase appears light, the aluminium-rich phase appears dark, and the tensile axis is vertical in these and all subsequent photomicrographs. The longitudinal marker lines provide clear evidence for grain boundary sliding at this elongation, as at the Zn–Zn intercrystalline boundaries labelled A in Fig. 1a and the Zn–Al interphase boundary labelled B in Fig. 1b.

Measurements of the boundary offsets led to an average offset, perpendicular to the tensile axis, of $\bar{w} \simeq 0.22\,\mu m$. Using Equation 2 with $\phi = 1.5$, this value of $\bar{w}$ gives $\xi \simeq 32 \pm 9\%^\dagger$; these values, and subsequent results, are summarized in Table II.

Similar surface features were observed at 35% elongation on the specimen tested at $1.33 \times 10^{-3}\,sec^{-1}$. Fig. 2 shows two examples, and there is clear evidence for sliding at the Zn–Zn intercrystalline boundaries labelled A, B and C in Fig. 2b. Close inspection of this

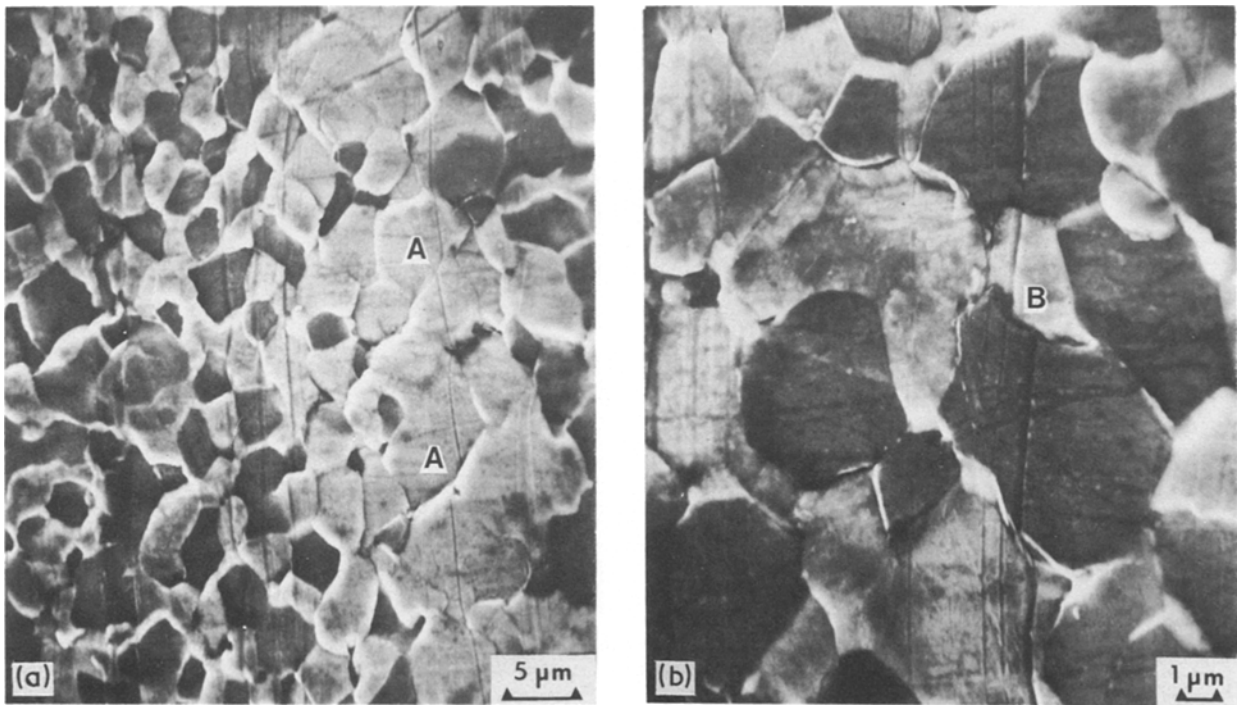

Figure 1 (a, b) Typical areas within the gauge length of the specimen tested at an initial strain rate of $1.33 \times 10^{-2}\,sec^{-1}$ to an elongation of 35%. Sharp offsets are visible in the longitudinal marker lines at A and B.

*Equation 3 contains a factor of $(1 + \varepsilon_t)$ because the lengths of the longitudinal marker lines, used to estimate the final grain size, were elongated by a factor of $(1 + \varepsilon_t)$ due to grain boundary sliding and extension of the grains.

†The error bars on ξ incorporate both the error on $\bar{w}$ and the uncertainty in $\bar{L}$.

TABLE II The magnitudes of the grain boundary offsets in longitudinal marker lines

Strain rate (sec^{-1})	Specimen elongation	$\bar{w}$ (μm)	ξ (%)	Specimen elongation	$\bar{w}$ (μm)	ξ (%)
1.33×10^{-2}	0 → 35%	~0.22	32 ± 9	196% → 234%	~0.20	71 ± 17
1.33×10^{-3}	0 → 35%	~0.16	23 ± 6	200% → 237%	~0.18	63 ± 15

specimen showed some evidence for the formation of striated bands, essentially perpendicular to the tensile axis, where one grain moves over an adjacent grain to expose a boundary facet. The formation of striated bands was noted earlier in Zn–22% Al [19, 27, 28], and in other superplastic materials [29–31], and it is generally associated with deformation at the lower testing strain rates. The early stages of striated band formation are visible in Fig. 2b at the boundary labelled A and at other boundaries such as D and E.

As indicated in Table II, the value of $\bar{w}$ was ~0.16 μm in this specimen, giving $\xi \simeq 23 \pm 6\%$.

Fig. 3 shows surface features on the specimen tested at 1.33×10^{-2} sec^{-1} to an elongation of 234% after repolishing and scribing at an elongation of 196%. Inspection of Fig. 3a shows that the grains are slightly elongated along the tensile axis, although the elongation of the individual grains is much smaller than the overall specimen elongation of > 200%. The surfaces of the individual grains appear a little rougher at this higher elongation, but this is due to the experimental difficulty of polishing the deformed sample at an elongation of ~200%. Grain boundary offsets are clearly visible in Figs 3b and c, and there are several examples of striated bands at the points labelled A and B. Offset measurements gave $\bar{w} \simeq 0.20\,\mu$m under this condition, and the mean linear intercept grain size at the termination of the test was $\bar{L}_f \simeq 3.7 \pm 0.6\,\mu$m. Thus, using Equation 3 with a relative increment of strain of $\varepsilon_t \simeq 13\%$ (equivalent to a total elongation from 196% to 234%), the value of ε is $\sim 71 \pm 17\%$.*

Fig. 4 shows representative surface features on the specimen deformed at 1.33×10^{-3} sec^{-1} to an elongation of 237%. Again, there is some evidence for elongation of individual grains along the tensile axis, as in Fig 4a. The photomicrographs show striated bands as at A in Fig. 4b and rotation of some of the smaller grains as at the grain labelled B in Fig. 4c. Measurements on this specimen gave $\bar{w} \simeq 0.18\,\mu$m and, since the value of $\bar{L}_f$ was also determined as $3.7 \pm 0.6\,\mu$m and $\varepsilon_t \simeq 13\%$, the value of ξ was estimated as $\sim 63 \pm 15\%$.

It has been established that the Zn–22% Al alloy shows extensive internal cavitation when pulled to fracture at high temperatures [36–38], and cavitation occurs also in this alloy when the purity is very high

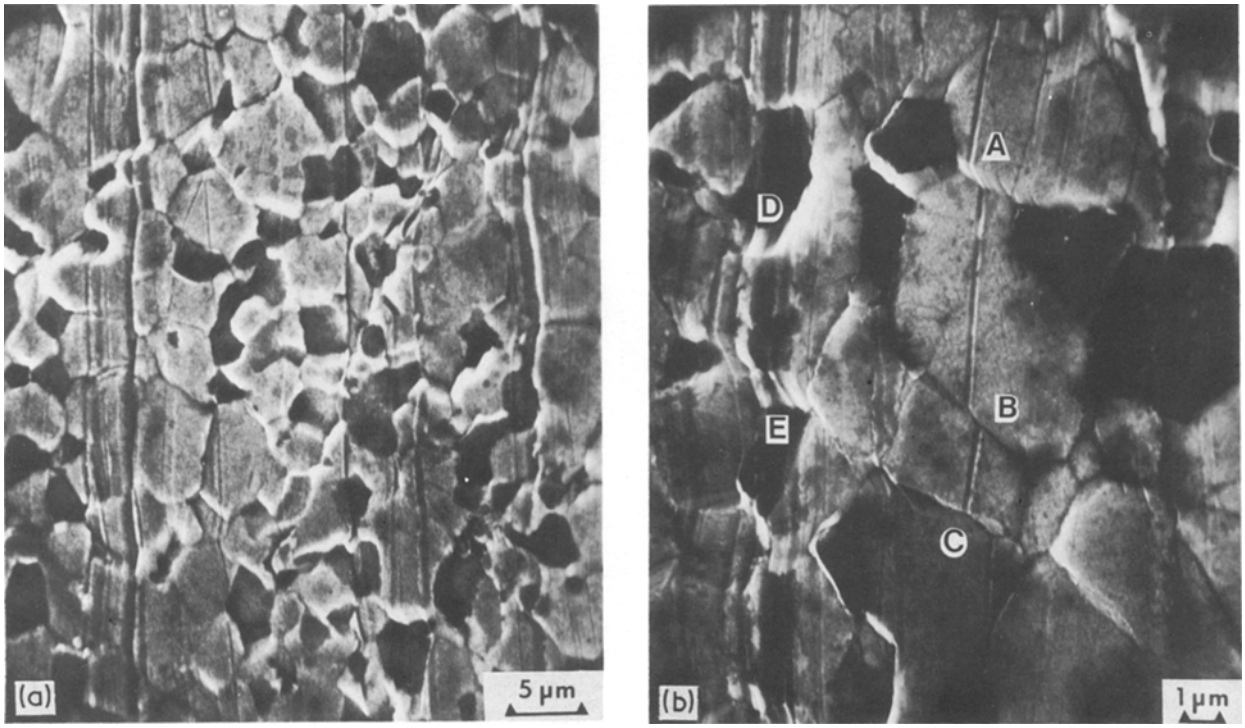

Figure 2 (a, b) Typical areas within the gauge length of the specimen tested at an initial strain rate of 1.33×10^{-3} sec^{-1} to an elongation of 35%. Sliding offsets are visible at the Zn–Zn intercrystalline boundaries labelled A, B and C, and there are striated bands at the boundaries labelled A, D and E.

*It has been established that grain growth occurs in many superplastic materials during testing, and there is both a natural grain coarsening due to the effect of temperature and a deformation-induced coarsening due to the occurrence of superplasticity [32–34]. If grain growth is extensive, Equation 3 is no longer valid because the value of $\bar{L}_f$, measured along the tensile axis after testing, includes not only the effect of specimen elongation but also the effect of concurrent grain growth. In the present experiments, the use of Equation 3 is justified for two reasons. First, it was established earlier that there is very little grain growth in Zn–22% Al when testing in Region II [35]. Second, the relative increment of strain between scribing and taking offset measurements was only ~13% at the higher elongation so that the effect of grain growth is necessarily extremely small.

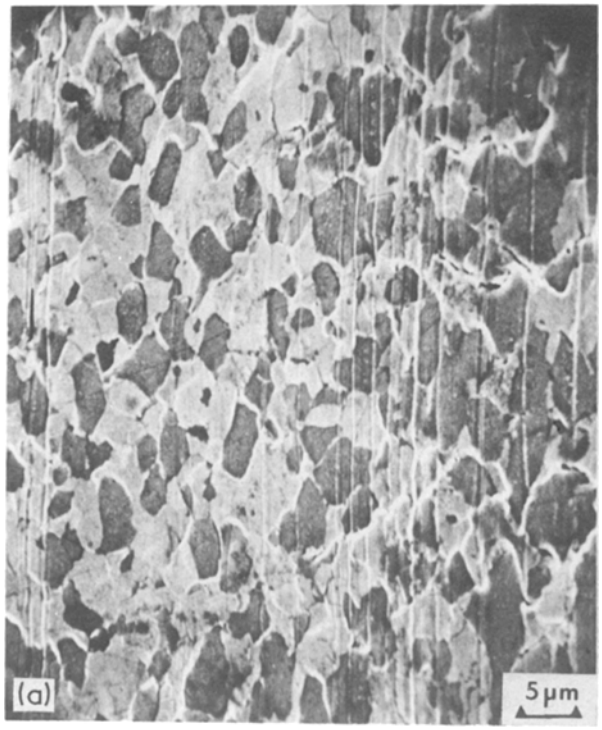

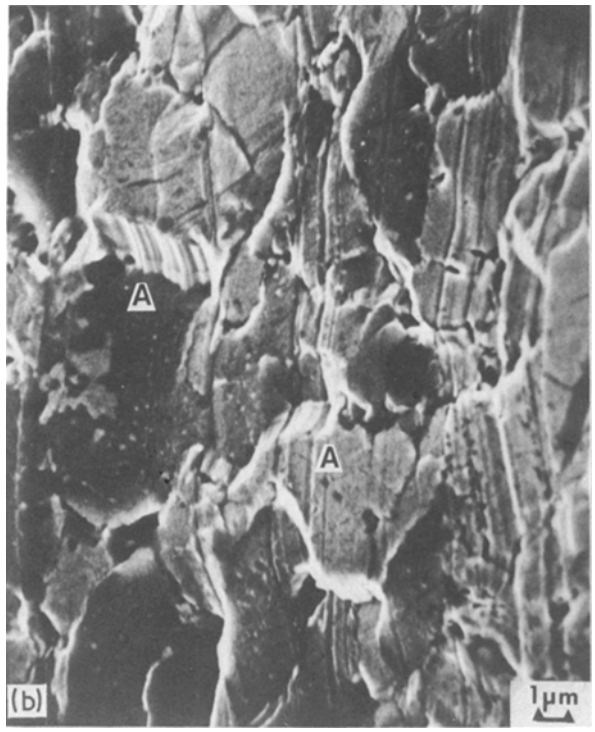

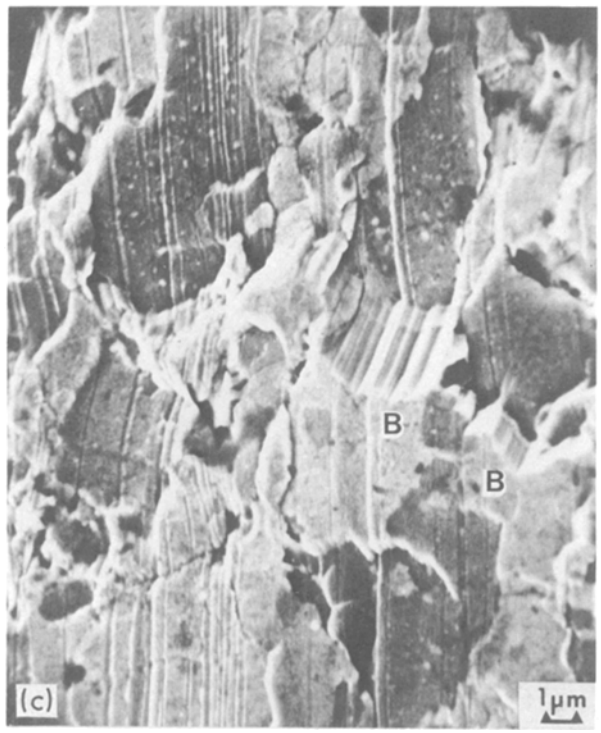

Figure 3 (a–c) Typical areas within the gauge length of the specimen tested at an initial strain rate of $1.33 \times 10^{-2}\,\text{sec}^{-1}$ to an elongation of 24% after repolishing at 196%. Striated bands are visible at the boundaries labelled A and B.

(~ 15 p.p.m. impurities) [39] so that cavity formation cannot be attributed solely to the presence of impurities. Fig. 4d shows an example, at point C, of the opening of a cavity around the perimeter of a very small aluminium-rich grain. This suggests that, at least in Zn–22% Al, cavity formation may be enhanced at the Zn–Al interfaces by an inhomogeneous distribution of grain sizes and especially by the presence of some very small grains (in this case, ~ 1 μm in diameter).

3.2. The variation of sliding with type of interface

Following the procedure adopted earlier by Shariat *et al.* [20], sliding was recorded in terms of both the magnitude of the offset and the type of interface. Table III summarizes the data for the three boundary types in Zn–22% Al, where $\bar{w}_i$ is the average offset for a specific type of interface. Thus, at 35% elongation for the specimen tested at $1.33 \times 10^{-2}\,\text{sec}^{-1}$, the values of $\bar{w}_i$ were ~ 0.20, ~ 0.28 and ~ 0.16 μm for the Zn–Al, Zn–Zn and Al–Al interfaces, respectively.

Inspection of Table III shows a general consistency in the values of $\bar{w}_i$: the average sliding offset tends to be highest at the Zn–Zn interfaces, slightly lower at the Zn–Al interfaces, and it is usually lowest at the Al–Al interfaces. Furthermore, this trend is evident under all experimental conditions except at the slower strain rate and higher elongation where the value of $\bar{w}_i$ at the Al–Al interfaces appears anomalously high.

The complete experimental data are plotted in the form of histograms in Figs 5 and 6 for the faster and slower strain rates, respectively. Figs 5a and 6a are for the lower elongation (35%), while Figs 5b and 6b are for the higher elongation (~ 235%); in each plot the histogram shows the relative contribution of sliding (as a percentage of the total amount) in 0.1 μm increments of w for the Zn–Zn, Zn–Al and Al–Al boundaries and also for the total number of boundaries, respectively.

4. Discussion

4.1. The significance of grain boundary sliding at high specimen elongations

There are divergent opinions concerning the role of grain boundary sliding at high elongations in Region II in the superplastic Zn–22% Al alloy and, by implication, in all superplastic materials. On the one hand,

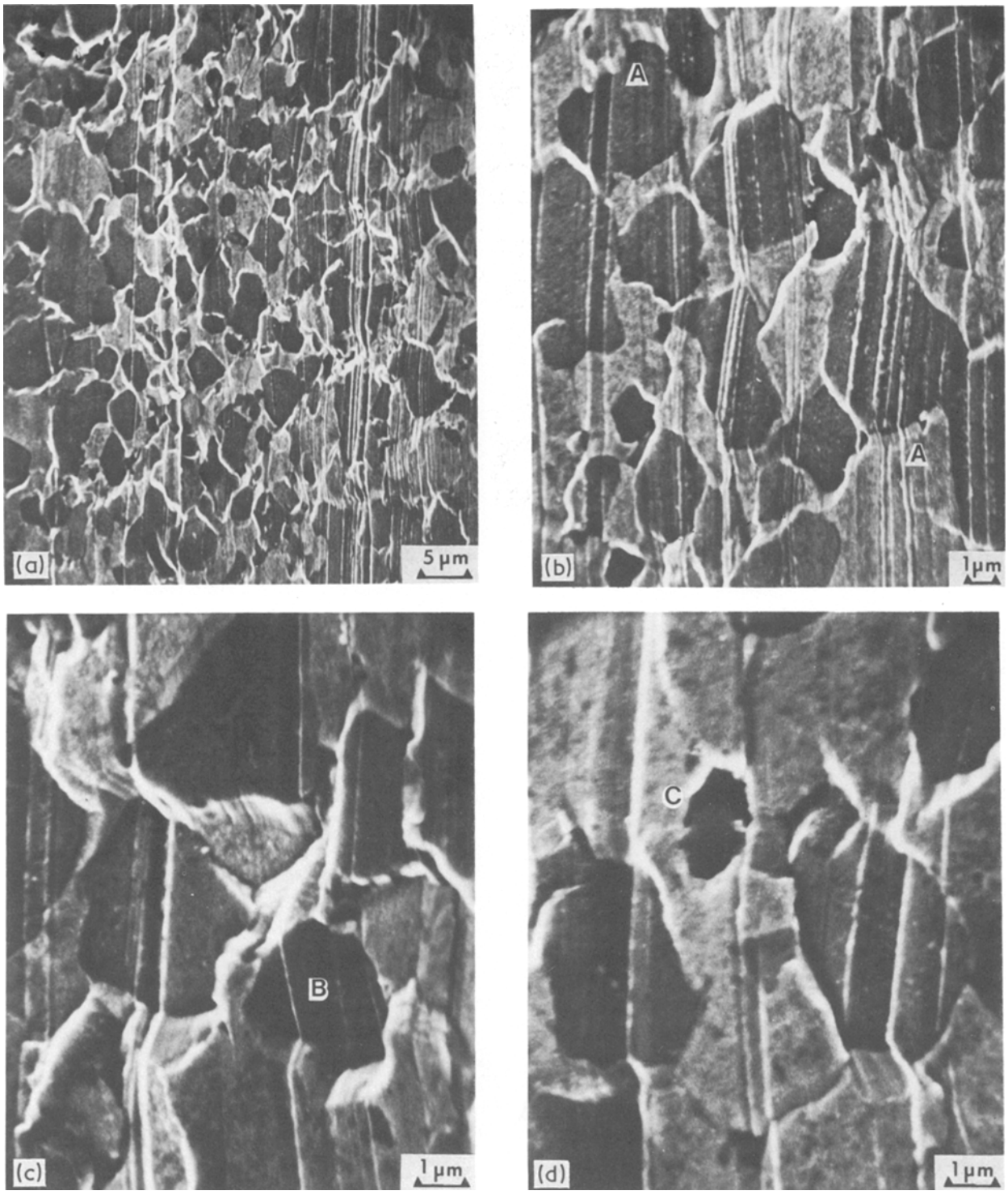

Figure 4 (a–d) Typical areas within the gauge length of the specimen tested at an initial strain rate of 1.33×10^{-3} sec^{-1} to an elongation of 237% after repolishing at 200%. Striated bands are visible at A, there is an example of rotation of a smaller grain at B, and a cavity is opening around the perimeter of a very small aluminium-rich grain at C.

TABLE III The variation of grain boundary offsets with type of boundary

Strain rate (sec^{-1})	Specimen elongation	Type of boundary	$\bar{w}_i$ (μm)	Specimen elongation	Type of boundary	$\bar{w}_i$ (μm)
1.33×10^{-2}	0 → 35%	Zn–Al	~0.20	196% → 234%	Zn–Al	~0.19
		Zn–Zn	~0.28		Zn–Zn	~0.26
		Al–Al	~0.16		Al–Al	~0.13
1.33×10^{-3}	0 → 35%	Zn–Al	~0.16	200% → 237%	Zn–Al	~0.16
		Zn–Zn	~0.16		Zn–Zn	~0.23
		Al–Al	~0.15		Al–Al	~0.20

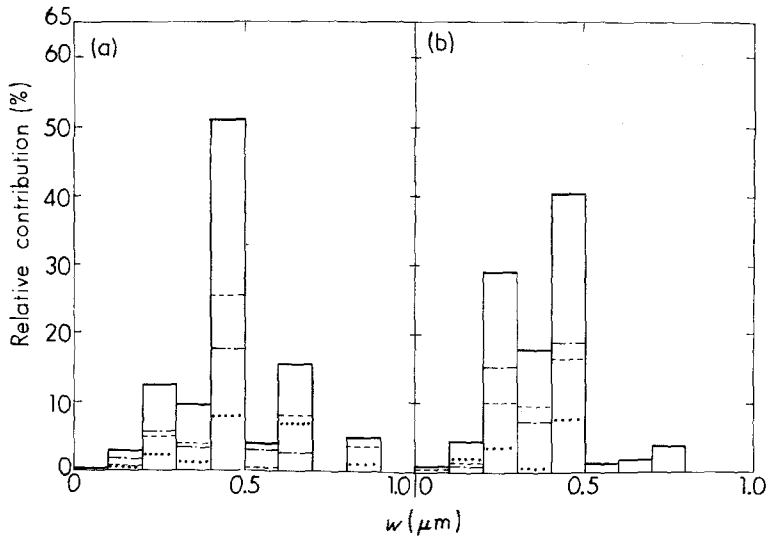

Figure 5 Relative contribution (as a percentage) against value of the offset perpendicular to the stress axis, w, for the specimen tested at 473 K and an initial strain rate of 1.33×10^{-2} sec^{-1} to elongations of (a) 35% and (b) 234% after a repolish at 196%. Boundary type: (– – –) Zn–Zn, (—·—) Zn–Al, (···) Al–Al, (——) total.

Shariat *et al.* [20] obtained very low values for ξ at an elongation of 100% ($\xi \simeq 11 \pm 5\%$) but concluded that, because of experimental difficulties in the procedure adopted for determining ξ, there was no true diminution in the sliding contribution. On the other hand, Motohashi and Shibata [21] postulated that sliding was important in the Zn–22% Al alloy only in the very early stages of deformation, up to elongations of $\sim 50\%$, and thereafter sliding decreased in importance as the rate-controlling mechanism changed to elongation of the zinc-rich phase.

The present results support the conclusions of Shariat *et al.* [20], and they demonstrate that grain boundary sliding remains important during superplastic flow up to elongations of $> 200\%$. Inspection of Table II shows that, within the accuracy of the measurements, the individual values of ξ are mutually consistent both at low elongations (up to 35%) and after an increment of strain at high elongations (up to $\sim 235\%$). By inference, it is reasonable to conclude that sliding is the dominant deformation mode throughout the high elongations inherent in the superplastic Region II.

The values of ξ obtained in this programme at 35% elongation appear rather low, especially at the strain rate of 1.33×10^{-2} sec^{-1} which, according to earlier experimental data [24], is near to the center of Region II. Thus, the present results give $\xi \simeq 32\%$ at this strain rate, whereas Table I shows that earlier results on Zn–22% Al, also tested in Region II, gave $\xi \simeq 60\%$ in two independent experiments [18, 19]. This difference is attributed primarily to the higher elongation employed in this work ($\sim 35\%$) which contrasts with the earlier measurements taken at an elongation of only 20%. The lower values of ξ in the present work may arise also in part because of the lower testing temperature (473 K instead of 523 K [18, 19]) and the slightly larger grain size ($\bar{L} \simeq 3.0\,\mu$m instead of $\bar{L} \simeq 1.8\,\mu$m [18] and $\sim 1.6\,\mu$m [19], respectively).

Motohashi and Shibata [21] reported a value of $\xi \simeq 80\%$ in Zn–22% Al at an elongation of 20%. However, this value is incorrect because they followed the experimental procedure described in an early review on methods of measuring ξ in high-temperature creep [40] and the review erroneously included a factor of $(1 + \varepsilon_t)$ in Equation 2; although this error was subsequently noted by Gittins [41], the correction appears to have been overlooked by Motohashi and Shibata [21]. When the correct Equation 2 is used in their calculation, the value of ξ is reduced to $\sim 67\%$ which is consistent with the two earlier investigations on Zn–22% Al at the same elongation [18, 19].

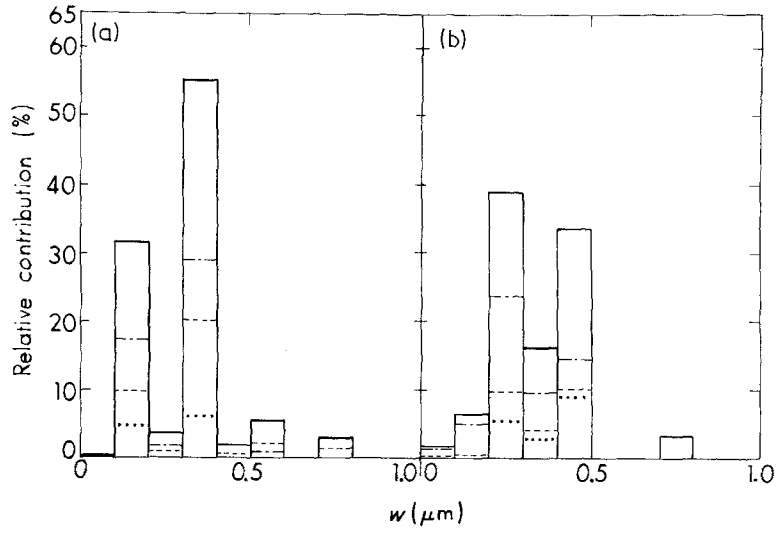

Figure 6 Relative contribution (as a percentage) against value of the offset perpendicular to the stress axis, w, for the specimen tested at 473 K and an initial strain rate of 1.33×10^{-3} sec^{-1} to elongations of (a) 35% and (b) 237% after a repolish at 200%. Boundary type: (– – –) Zn–Zn, (—·—) Zn–Al, (···) Al–Al, (——) total.

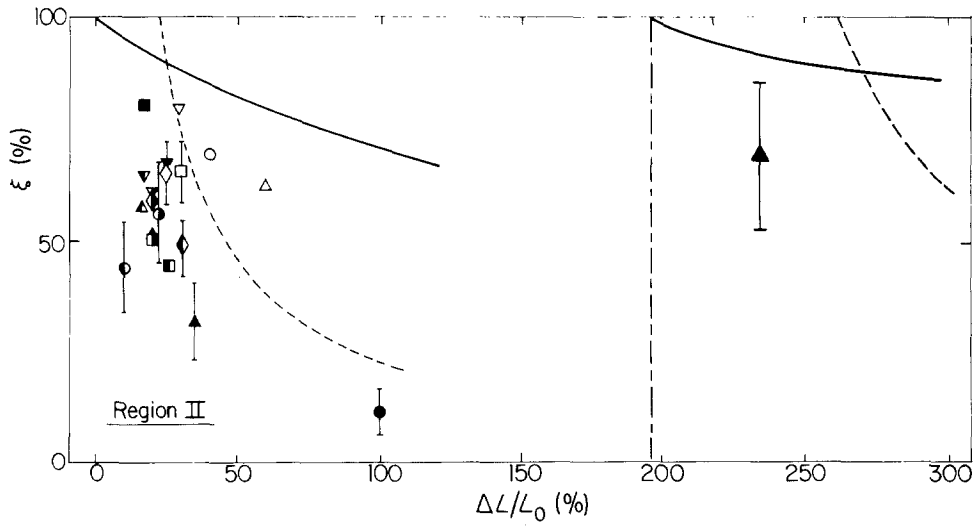

Figure 7 The contribution of grain boundary sliding, ξ, against the elongation at which the offset measurements were recorded, $\Delta L/L_0$, for various superplastic alloys in Region II. The solid and broken curves show the effect of limitations on the experimental procedures for measuring ξ: (——) effect of new surface material, (– – –) effect of limit on $\bar{w}/\bar{L}$. (○) Al–33% Cu [4], (□) Al–6.3% Mg–0.5% Mn [5], (△) Al–9% Zn–1% Mg [6], (▽) Al–11% Zn–0.9% Mg–0.3% Zr [7], (◇) Al–11% Zn–0.9% Mg–0.3% Zr [8], (◐) Cu–2.8% Al–1.8% Si–0.4% Co [9], (◧) Cu–21% Zn–4% Al [10], (◭) Mg–4.3% Al–1.0% Zn–0.4% Mn [11], (▽) Mg–33% Al [12], (◇) Mg–1.5% Mn–0.3% Ce [13], (◑) Pb–62% Sn [15], (◨) Pb–62% Sn [16], (◭) Zn–0.4% Al [17], (▼) Zn–22% Al [18], (◇) Zn–22% Al [19], (●) Zn–22% Al [20], (■) Zn–22% Al [21], (▲) Zn–22% Al (this investigation), (▼) Zn–0.9% Cu–0.6% Mn [22].

Thus, all of the experimental values reported for ξ in the Zn–22% Al eutectoid alloy are mutually consistent.

Finally, it should be noted that Motohashi and Shibata [21] suggested that the dominant deformation process at specimen elongations above $\sim 100\%$ is elongation of the zinc-rich phase along the tensile axis. This suggestion is not supported by the present microscopic evidence since, although there is some elongation of the individual phases as in Figs 3a and 4a, the percentage elongation of each phase is significantly smaller than the overall elongation of the specimen.

4.2. The limitations on measurements of ξ

As noted by Shariat *et al.* [20], there are two significant limitations inherent in the experimental procedures for measuring ξ. To document the significance of these limitations, Fig. 7 plots all the values reported for ξ in Region II, as documented in Table I, as a function of the specimen elongation at which the measurements were taken.*

The first limitation arises because new grains are exposed at the specimen surface during deformation and these grains do not contain the scribed marker lines. Assuming constant volume and a specimen with cylindrical or square cross-section, the ratio of the surface area at an elongation of $\Delta L/L_0$ to the original surface area is $(1 + \Delta L/L_0)^{0.5}$. Thus, there is an upper limit on experimental measurements of the sliding contribution, ξ_{max}, which is given by

$$\xi_{max} = \left(1 + \frac{\Delta L}{L_0}\right)^{-0.5} \quad (4)$$

Equation 4 represents the effect of new surface material and it is shown by the solid line up to $\sim 100\%$ in Fig. 7. For example, this effect imposes an experimental limit of $\xi_{max} \simeq 71\%$ at a specimen elongation of 100%.

The second limitation is due to the physical restriction on the maximum value of $\bar{w}/\bar{L}$ in Equation 2. If, on average, a longitudinal marker line intersects a grain boundary at the mid-point, it was demonstrated by Shariat *et al.* [20] that the maximum offset is of the order of $\bar{w} \simeq 0.15\,\bar{L}$. This limitation has a major effect on measurements of ξ at high specimen elongations, as shown by the broken line extending up to $\sim 100\%$ in Fig. 7. For example, this limitation restricts the maximum measured value of ξ to $\sim 22\%$ at a specimen elongation of 100%.

The cumulative effect of these two limitations is reduced to zero whenever a specimen is repolished during testing. In Fig. 7, the limiting lines and the experimental value of ξ are shown also for the specimen tested at $1.33 \times 10^{-2}\ \text{sec}^{-1}$ and repolished at an elongation of 196%.

In principle, all experimental values of ξ are expected to lie below the limiting values given by the solid and broken lines in Fig. 7. However, inspection shows that three values reported for ξ exceed the limits imposed by the magnitude of $\bar{w}/\bar{L}$.

For two of these materials, the Al–11% Zn–0.9% Mg–0.3% Zr alloy tested by Matsuki *et al.* [7] and the Al–33% Cu eutectic alloy tested by Hori *et al.* [4], the values of ξ were obtained by incorrectly including the factor of $(1 + \varepsilon_t)$ in Equation 2. When corrected, these values of ξ are reduced from $\sim 80\%$ and $\sim 70\%$ to $\sim 61\%$ and $\sim 50\%$, respectively, so that they both lie below the limiting line.

*The datum points plotted in Fig. 7 are the values reported for ξ by each set of investigators, and there has been no attempt to standardize these values because of the use of different measuring procedures. No datum point is shown for the investigation on Pb–62% Sn by Dingley [14] because the elongation was not specified.

The third experimental point lying above the line, for the Al–9% Zn–1% Mg alloy tested by Matsuki *et al.* [6], is unique because it is the only value of ξ in Fig. 7 obtained by using a series of inert particles to form an internal longitudinal marker line. Although this procedure has no limitation due to new material at the surface, provided the new material also contains the marker line, it should encounter the same restriction due to the physical limit on the value of $\bar{w}/\bar{L}$. Inspection of the published data suggests that the high value of ξ (63%) is due to the use of a specimen containing a single marker rather than the multiplicity of markers employed in the other investigations. As a result, it was possible for Matsuki *et al.* [6] to record very large sliding offsets, and therefore very large values of $\bar{w}$, even when the marker no longer impinged on a single grain boundary: an example of a large offset associated with more than one grain boundary, and occurring at an elongation of 60%, is shown near the left edge of their Fig. 4b. Under these conditions, the limitations indicated in Fig. 7 no longer apply.

4.3. The dependence of sliding on the type of interface

The values of $\bar{w}_i$ in Table III support the earlier conclusion by Shariat *et al.* [20] that maximum sliding occurs at the Zn–Zn boundaries, with less sliding at the Zn–Al interphase boundaries and, in general, minimum sliding at the Al–Al interfaces. This trend appears to be essentially independent of strain rate and specimen elongation.

The histograms in Figs 5 and 6 are also consistent with the earlier results obtained in Region II at 100% elongation by Shariat *et al.* [20]. As previously, the maximum sliding contribution is due to offsets in the vicinity of 0.5 μm at an initial strain rate of $1.33 \times 10^{-2}\,\text{sec}^{-1}$, and there are no recorded offsets larger than 1.0 μm. An important additional observation is that the histograms are very similar at both the low (35%) and high ($\sim$235%) elongations, thereby confirming that sliding continues in a similar manner throughout superplastic deformation.

4.4. The implications of these results

As shown in Table II, the experimental values of ξ are essentially identical at two strain rates differing by one order of magnitude. Microduplex alloys such as the Zn–22% Al eutectoid generally exhibit a superplastic Region II extending over up to almost three orders of magnitude of strain rate [24], and the similarity in the values of ξ at two different strain rates in Region II provides some support for the suggestion that superplastic behaviour in these alloys is controlled by a single deformation process.

Many of the experimental observations in superplasticity are necessarily conducted at low total elongations. For example, experiments were reported recently [42] in which coherent twin boundaries were used to provide quantitative information on the extent of intragranular slip in the superplastic deformation of a quasi-single phase copper-based alloy. In that work, the dislocation densities in coherent twin boundaries were measured in Region II up to elongations of 40%, and it was concluded that (i) intragranular slip is of relatively minor importance in superplastic deformation and (ii) the rate-controlling mechanism is grain boundary sliding due to the movement of dislocations along the grain boundaries. Although these experiments were undertaken at a relatively low specimen elongation, the present results provide additional support for this type of observation because the deformation process in Region II appears to remain essentially constant up to high elongations.

Finally, the present results have implications for cavitation failure in superplastic alloys. Grain boundary sliding is considered to be intimately involved in the process of cavity nucleation in superplastic materials, and high-voltage transmission electron microscopy has shown that cavities may nucleate under superplastic conditions within elongations of the order of 10% [43]. However, since the present results show that the contribution from grain boundary sliding remains high up to large elongations, it is anticipated that there will be a continuous nucleation of cavities throughout the superplastic deformation. This is consistent both with some experimental observations [44–46] and with a theoretical model for cavitation in superplasticity [47].

5. Summary and conclusions

1. Experiments were performed to measure the contribution from grain boundary sliding to the total strain in the Zn–22% Al eutectoid alloy at both low (35%) and high ($\sim$235%) elongations after deformation at two different strain rates in Region II. The results show that, within the accuracy of the measurements, there is a large sliding contribution at both elongations and at both strain rates.

2. In general, the sliding offsets are a maximum at the Zn–Zn boundaries, there is less sliding at the Zn–Al interfaces, and the offsets are a minimum at the Al–Al boundaries. By recording both the magnitude of the boundary offset and the type of interface, it is shown that the distributions of the magnitudes of the sliding offsets are similar at both low (35%) and high ($\sim$235%) elongations.

3. It is concluded that grain boundary sliding is an important deformation process in superplasticity in Region II, and that sliding remains important even when the overall specimen elongation is very high.

4. It is further concluded that experimental observations of the deformation behaviour in superplastic materials at low specimen elongations (up to 50%) provide meaningful information on the behaviour at much higher (superplastic) elongations.

Acknowledgement

This work was supported by the National Science Foundation under Grant No. DMR-8503224.

References

1. D. A. WOODFORD, *Trans. ASM* **62** (1969) 291.
2. F. A. NICHOLS, *Acta Metall.* **28** (1980) 663.
3. A. H. CHOKSHI and T. G. LANGDON, in "Superplasticity", edited by B. Baudelet and M. Suéry (Centre National de la Recherche Scientifique, Paris, 1985) p. 2.1.
4. S. HORI, N. FURUSHIRO and S. KAWAGUCHI, *J.*

Jpn Inst. Light Metals **25** (1975) 361.
5. R. Z. VALIEV, O. A. KAIBYSHEV, M. Kh. RABINOVICH, Yu. P. TIMOSHENKO and O. L. CHISTOVA, *Fiz. Metal. Metalloved.* **51** (1981) 615.
6. K. MATSUKI, H. MORITA, M. YAMADA and Y. MURAKAMI, *Metal Sci.* **11** (1977) 156.
7. K. MATSUKI, Y. UENO and M. YAMADA, *J. Jpn Inst. Metals* **38** (1974) 219.
8. K. MATSUKI, N. HARIYAMA and M. TOKIZAWA, *ibid.* **45** (1981) 935.
9. S.-A. SHEI and T. G. LANGDON, *J. Mater. Sci.* **16** (1981) 2988.
10. V. K. PORTNOY and V. A. KOZHANOV, *Fiz. Metal. Metalloved.* **55** (1983) 592.
11. C. PUQUAN and Z. MIN, in "Strength of Metals and Alloys (ICSMA7)", Vol. 2, edited by H. J. McQueen, J.-P. Baïlon, J. I. Dickson, J. J. Jonas and M. G. Akben (Pergamon, Oxford, 1985) p. 817.
12. D. LEE, *Acta Metall.* **17** (1969) 1057.
13. R. Z. VALIEV and O. A. KAIBYSHEV, *Phys. Status Solidi (a)* **44** (1977) 65.
14. D. J. DINGLEY, in "Scanning Electron Microscopy" (IIT Research Institute, Chicago, 1970) p. 331.
15. R. B. VASTAVA and T. G. LANGDON, *Acta Metall.* **27** (1979) 251.
16. N. FURUSHIRO and S. HORI, *Scripta Metall.* **13** (1979) 653.
17. O. A. KAIBYSHEV, R. Z. VALIEV and V. V. ASTANIN, *Phys. Status Solidi (a)* **35** (1976) 403.
18. D. L. HOLT, *Trans. Metall. Soc. AIME* **242** (1968) 25.
19. I. I. NOVIKOV, V. K. PORTNOY and T. E. TERENTIEVA, *Acta Metall.* **25** (1977) 1139.
20. P. SHARIAT, R. B. VASTAVA and T. G. LANGDON, *ibid.* **30** (1982) 285.
21. Y. MOTOHASHI and T. SHIBATA, *J. Fac. Eng. Ibaraki Univ.* **30** (1982) 49.
22. K. MATSUKI, N. HARIYAMA, M. TOKIZAWA and Y. MURAKAMI, *Metal Sci.* **17** (1983) 503.
23. R. I. KUZNETSOVA, N. N. ZHUKOV, O. A. KAIBYSHEV and R. Z. VALIEV, *Phys. Status Solidi (a)* **70** (1982) 371.
24. F. A. MOHAMED and T. G. LANGDON, *Acta Metall.* **23** (1975) 117.
25. T. G. LANGDON, *Metall. Trans.* **3** (1972) 797.
26. R. L. BELL, C. GRAEME-BARBER and T. G. LANGDON, *Trans. Metall. Soc. AIME* **239** (1967) 1821.
27. I. I. NOVIKOV, V. K. PORTNOY and V. S. LEVCHENKO, *Acta Metall.* **29** (1981) 1077.
28. P. SHARIAT, R. B. VASTAVA and T. G. LANGDON, in "Microstructural Science", Vol. 10, edited by W. E. White, J. H. Richardson and J. L. McCall (Elsevier, New York, 1982) p. 337.
29. S. W. ZEHR and W. A. BACKOFEN, *Trans. ASM* **61** (1968) 300.
30. G. L. DUNLOP and D. M. R. TAPLIN, *J. Mater. Sci.* **7** (1972) 316.
31. V. E. IVANOV, I. I. PAPIROV, G. F. TIKHINSKII, V. S. SHOKUROV, L. A. KORNIENKO and A. A. NIKOLAENKO, *Dokl. Akad. Nauk SSSR* **256** (1981) 73.
32. D. S. WILKINSON and C. H. CÁCERES, *Acta Metall.* **32** (1984) 1335.
33. M. C. PANDEY, J. WADSWORTH and A. K. MUKHERJEE, *Scripta Metall.* **19** (1985) 1229.
34. O. N. SENKOV and M. M. MYSHLYAEV, *Acta Metall.* **34** (1986) 97.
35. F. A. MOHAMED, M. M. I. AHMED and T. G. LANGDON, *Metall. Trans. A* **8** (1977) 933.
36. H. ISHIKAWA, D. G. BHAT, F. A. MOHAMED and T. G. LANGDON, *ibid.* **8** (1977) 523.
37. M. M. I. AHMED, F. A. MOHAMED and T. G. LANGDON, *J. Mater. Sci.* **14** (1979) 2913.
38. D. W. LIVESEY and N. RIDLEY, *ibid.* **17** (1982) 2257.
39. D. A. MILLER and T. G. LANGDON, *Metall. Trans. A* **9** (1978) 1688.
40. R. N. STEVENS, *Trans. Metall. Soc. AIME* **236** (1966) 1762.
41. A. GITTINS, *ibid.* **239** (1967) 922.
42. L. K. L. FALK, P. R. HOWELL, G. L. DUNLOP and T. G. LANGDON, *Acta Metall.* **34** (1986) 1203.
43. R. G. FLECK, D. M. R. TAPLIN and C. J. BEEVERS, *ibid.* **23** (1975) 415.
44. D. W. LIVESEY and N. RIDLEY, *Metall. Trans. A* **13** (1982) 1619.
45. J. PILLING, *Mater. Sci. Tech.* **1** (1985) 461.
46. A. H. CHOKSHI, *Metall. Trans. A* **18** (1987) 63.
47. A. K. GHOSH, in "Deformation of Polycrystals: Mechanisms and Microstructures," edited by N. Hansen, A. Horsewell, T. Leffers and H. Lilholt (Risø National Laboratory, Roskilde, Denmark, 1981) p. 277.

Received 19 May
and accepted 22 July 1987